REPORT DOCUMENTATION PAGE

Form Approved
OMB NO. 0704-0188

Public Reporting burden for this collection of information is estimated to average 1 hour per response, including the time for reviewing instructions, searching existing data sources, gathering and maintaining the data needed, and completing and reviewing the collection of information. Send comment regarding this burden estimates or any other aspect of this collection of information, including suggestions for reducing this burden, to Washington Headquarters Services, Directorate for information Operations and Reports, 1215 Jefferson Davis Highway, Suite 1204, Arlington, VA 22202-4302, and to the Office of Management and Budget, Paperwork Reduction Project (0704-0188,) Washington, DC 20503.

1. AGENCY USE ONLY (Leave Blank)	2. REPORT DATE 06-30-2006	3. REPORT TYPE AND DATES COVERED 15 Feb 02 – 31 Mar 06

4. TITLE AND SUBTITLE	5. FUNDING NUMBERS
Numerical Simulation of Stall and Stall Control in Axial and Radial Compressors	Proposal No. 43737-EG
6. AUTHOR(S) Chen, J.P., Webster, R.S., Hathaway, M.D., Herrick, G.P., Skoch, G.J.	DAAD19-02-1-0019

7. PERFORMING ORGANIZATION NAME(S) AND ADDRESS(ES) Mississippi State University Starkville, MS 39759	8. PERFORMING ORGANIZATION REPORT NUMBER

9. SPONSORING / MONITORING AGENCY NAME(S) AND ADDRESS(ES) U. S. Army Research Office P.O. Box 12211 Research Triangle Park, NC 27709-2211	10. SPONSORING / MONITORING AGENCY REPORT NUMBER 43737.1-EG

11. SUPPLEMENTARY NOTES
The views, opinions and/or findings contained in this report are those of the author(s) and should not be construed as an official Department of the Army position, policy or decision, unless so designated by other documentation.

12 a. DISTRIBUTION / AVAILABILITY STATEMENT Approved for public release; distribution unlimited.	12 b. DISTRIBUTION CODE

13. ABSTRACT (Maximum 200 words)

The performance of gas turbine engines is limited by compressor stall, and further exacerbated by combat conditions. Stall control technologies developed at the Army Research Laboratory (ARL) Vehicle Technology Directorate (VTD) and NASA Glenn Research Center (GRC) have demonstrated the effectiveness of steady tip injection to increase the stable operating range of high-speed axial and centrifugal compressors. A major element lacking in the development of the stall control technology is a fundamental understanding of the fluid mechanic processes of stall inception, and how stall is mitigated by the stall control technology to achieve increased compressor stall range. Such understanding is essential for providing improved design guidance in implementing stall control technology in engines. As such, in parallel with the engine demonstrator tests we are generating time-accurate, full-annulus, three-dimensional Navier-Stokes code simulations of single-stage axial and centrifugal compressors for which detailed experimental data are available, both with and without stall control technology. This paper presents results of the TURBO simulations, which show predicted range extension with stall control technology compared to measurements, and characteristics of the compressor flow field with and without stall control technology.

14. SUBJECT TERMS CFD, turbomachinery, compressor, stall, control			15. NUMBER OF PAGES 13
			16. PRICE CODE

17. SECURITY CLASSIFICATION OR REPORT UNCLASSIFIED	18. SECURITY CLASSIFICATION ON THIS PAGE UNCLASSIFIED	19. SECURITY CLASSIFICATION OF ABSTRACT UNCLASSIFIED	20. LIMITATION OF ABSTRACT UL

NSN 7540-01-280-5500

Standard Form 298 (Rev.2-89)
Prescribed by ANSI Std. 239-18
298-102

Enclosure 1

Numerical Simulation of Stall and Stall Control in Axial and Radial Compressors

Jenping Chen

Roberts S. Webster

Mississippi State University
Starkville, MS

University of Tennessee
Chattanooga, TN

Michael D. Hathaway, Gregory P. Herrick, Gary J. Skoch,

Vehicle Technology Directorate, Army Research Laboratory
Cleveland, OH

Abstract

The performance of gas turbine engines is limited by compressor stall, and further exacerbated by combat conditions. Stall control technologies developed at the Army Research Laboratory (ARL) Vehicle Technology Directorate (VTD) and NASA Glenn Research Center (GRC) have demonstrated the effectiveness of steady tip injection to increase the stable operating range of high-speed axial and centrifugal compressors. A major element lacking in the development of the stall control technology is a fundamental understanding of the fluid mechanic processes of stall inception, and how stall is mitigated by the stall control technology to achieve increased compressor stall range. Such understanding is essential for providing improved design guidance in implementing stall control technology in engines.

As such, in parallel with the engine demonstrator tests we are generating time-accurate, full-annulus, three-dimensional Navier-Stokes code simulations of single-stage axial and centrifugal compressors for which detailed experimental data are available, both with and without stall control technology. This paper presents results of the TURBO simulations, which show predicted range extension with stall control technology compared to measurements, and characteristics of the compressor flow field with and without stall control technology.

Introduction

Gas turbine engines are the prime movers in a large number of combat vehicles for the Army, Navy, and Air Force including surface ships, tanks, manned and unmanned fixed-wing and rotary-wing combat aircraft, and logistic aircraft. These engines must perform reliably in harsh operating arenas while maintaining a high degree of operational availability. The stable operating envelope of gas turbine engines is dictated in large part by the aerodynamic stability (tolerance to stall) of the engine compression system. Factors that reduce compression system tolerance to stall are erosion due to ingestion of debris during takeoff and landing from damaged and unimproved fields and during low-altitude maneuvers, increased clearances due to blade tip rubs during hard landings, and distorted intake flows during combat maneuvers or due to ingestion of hot gas during munitions firing. In addition, the increasing use of stealth technology is generating requirements that conceal engine intakes and

exhaust streams from direct observation, further reducing intake flow quality and thus degrading compressor stability.

Researchers at the ARL Vehicle Technology Directorate and NASA Glenn Research Center have developed compressor stall control technologies that have been successfully demonstrated in compressor component tests[1-6]. These stability enhancement technologies have been developed through parametric experimental studies. Their effectiveness is based on altering the unsteady flow field near the compressor blade tips[1-6]. However, there is a lack of fundamental understanding of the fluid mechanic processes of stall inception and how these stall control technologies mitigate stall to achieve increased compressor stability. Improved understanding of the stall inception process will guide the further development of stall control devices and of compressor blading with increased tolerance to stall, thereby expanding the operational envelope of military gas turbine engines.

During the last ten years steady-flow computational simulations have provided an increasingly accurate prediction of the flow up to the point of compressor stall. However, attempts to study stall through unsteady simulations of a subset of the blades in a compressor blade row[7] or through reduced-order unsteady flow models[8, 9] have met with limited success. Since the temporal flow field variations that occur during stall inception are not harmonics of blade passing frequency the unsteady flow in every blade passage within a blade row must be simulated in order to study the transition from a steady flow state into the unsteady stalled flow state. Such simulations have been done two-dimensionally[10], but stall and the instabilities leading to stall are inherently three-dimensional unsteady phenomena, which occur at non-integral multiples of blade passing frequency. Predicting stall phenomena thus requires three-dimensional unsteady full-annulus simulations, which is a daunting computational endeavor requiring considerable computational resources. To facilitate such, a building block approach has been adopted using progressively greater scope of simulations to boot strap from steady flow simulations, through unsteady phase-lag and partial annulus simulations[11, 12] to finally unsteady full-annulus simulations, presented herein, to investigate the stall inception process with and without stall control technology. Major improvements in the ability to accurately simulate *steady* flows near the blade tip in axial compressor rotors through improved gridding techniques[13], and concurrent improvements in the accuracy of an *unsteady* flow solver for turbomachinery blading (TURBO) through improvements in grid generation and turbulence modelling[14], as well as advancements in computational capability have made such simulations possible.

The TURBO code is fully parallelized and has been successfully used as a production code for unsteady simulations of near design point conditions of multistage compressors. The intent of the present effort is to validate the suitability of TURBO for use in simulating the unsteady stall inception process, both with and without stall control technology. The validation entails 3D viscous full-annulus unsteady simulations of both a high-speed axial and centrifugal compressor stage wherein experimental data are available both with and without stall control technology. The results will be used to investigate the stall inception process and mitigating effects of stall control technology, which are expected to provide insight into the causal link between compressor blade design parameters and the stable operating limit.

Problem and Computational Methodology

Stall detection schemes and stall controllers rely on the presence of small-amplitude stall precursive disturbances (which are measured with high-response transducers and form the inputs to stall warning and stall control systems). The uncontrolled growth of these disturbances leads to stall. We do not currently understand the causal link between these disturbances and the fluid mechanic processes occurring within the compressor blade row just prior to stall. Furthermore we don't understand the fundamental fluid mechanics of how stall control technology extends the stable operating range of a compressor. Determining this causal link and how stall control technology beneficially affects such to extend the stable operating range of a compressor are the key objectives of this effort.

Typical flow phenomena involved in rotating machinery can include shocks, vortices, separations, secondary flows, shock and boundary layer interactions, and turbulent wakes. Any CFD simulation of turbomachinery must be capable of resolving the multiple length and time scales found in these flows. The TURBO code, whose development has been supported by NASA, DOD, and industry, is a flow solver that approaches the goal of a high fidelity simulation of multistage turbomachinery flow physics[14].

The TURBO code was developed to simulate the highly complex flow fields generated by rotating machinery. This code is a finite volume, implicit scheme for unsteady, three-dimensional, compressible, viscous flows. It solves the Reynolds averaged Navier-Stokes equations. Flux vector splitting is used in evaluating flux Jacobians on the left hand side while Roe's flux difference splitting is used to form a higher-order TVD scheme for the evaluation of convective fluxes on the right hand side. Newton sub-iterations are applied to obtain a converged solution within one time step. Numerical instability problems can occur as the grids are clustered on the walls in order to resolve the viscous effects. Therefore, a modified two-pass scheme similar to Gauss-Seidel is used to reduce the errors brought about by the approximate factorization of the old two-pass scheme, and hence allow larger CFL numbers for the Navier Stokes type grids.

For implicit schemes, flux jacobians are needed to linearize the physical flux vectors, which contain both inviscid and viscous components. The viscous jacobians were done with a numerical formulation in the older versions of the code. Redundant computation of viscous fluxes had consumed almost one third of the entire computing time. To improve the performance, an analytical formulation was implemented. The result is a 30% reduction in CPU time and enhanced code robustness.

The steady Navier-Stokes Turbomachinery solver APNASA[15] is used to compute an initial guess at the time-accurate flow field for the TURBO code. Starting the

TURBO computation from this high quality initial flow field makes it easier to overcome the initial transient phase during the computation and in some cases results in an order of magnitude reduction in the CPU time that is required to reach a converged time-accurate solution[16]. This procedure is well demonstrated and is the standard method for beginning a time accurate calculation.

Both TURBO and APNASA use an advanced two-equation turbulence model that was developed specifically for turbomachinery flows by ICOMP at NASA Glenn Research Center[17]. This model has demonstrated superior ability to accurately simulate important viscous effects, such as shock/boundary layer interaction, in turbomachinery environments.

Computational issues that arise for this project include both portability and scalability of the flow solvers, as well as the spatial resolution and time steps needed for accurate simulations of stall characteristics. The parallel TURBO code is implemented in a portable, scalable form for distributed-memory parallel computers using MPI message passing[18]. The solution algorithm is an iterative implicit time-accurate scheme with characteristics-based finite-volume spatial discretization. The Newton sub-iterations are solved using a concurrent block-Jacobi symmetric Gauss-Seidel (BJ-SGS) relaxation scheme. Unsteady blade-row interaction is treated either by simulating full or periodic sectors of blade-rows, or by solving within a single passage for each row using phase-lag and wake-blade interaction approximations at boundaries. A scalable dynamic sliding-interface algorithm is used here, with an efficient parallel data communication between blade rows in relative motion.

The parallel code is implemented by a single-program multiple-data (SPMD) parallelization strategy. In this strategy, a single program is replicated for each processor and run with the data associated with a sub domain of the original computational domain. The parallel communication framework has been coded to support solution of problems using multi-block structured grids in which the block connectivity of the grid blocks is arbitrary. The original grids, one per blade passage, need to be partitioned before the execution of the flow solver. The grid partitioning is done with the preprocessor GUMBO[19], which features a graphical user interface. The approach to parallelization for large-scale complex problems is discussed in further detail in References 20-22. Portability has been demonstrated for numerous parallel platforms including T3E, IBM SP-3 and SP-4, Sun Enterprise ULTRA 10000, SGI-O2K and PCA Arrays, as well as workstation clusters. The parallel TURBO code to be used is an evolution of the sequential version that has been validated very extensively over the years. The parallel version has been validated by repeating selected flow cases previously validated using the sequential version.

To facilitate and expedite setup of a full-annulus simulation, the domain decomposition preprocessor GUMBO was modified so that the entire setup process can be done automatically. This process includes rotate-copying the grid and solution into a full-annulus, partitioning and renumbering the blocks, generating all boundary conditions and connectivity information. This improvement is significant in that it reduces the setup time for cases of this kind from days to hours.

Scalability studies have indicated linear or even super linear speedups were achievable as long as parallel efficiency maintained at 85% or above[11], with the parallel efficiency as a function of load balance and network capacity. On average the parallel efficiency for all the axial compressor simulations on the IBM SP-3 is above 90%. It is therefore assured that the calculations on these computers are highly scalable.

Results and Discussion

Stall control technology developed collaboratively by researchers at the Army Research Laboratory's Vehicle Technology Directorate and the NASA Glenn Research Center have been demonstrated to extend the stable operating range of both high speed axial and centrifugal compressors[1-6]. The stall control technology involves local discrete injection of high relative total pressure fluid to energize regions of low momentum fluid, which are believed to play a critical role in destabilizing the compressor. For axial compressors this entails injection of high relative total pressure fluid just upstream of the rotor tip leading edge at discrete locations around the annulus to energize the low momentum flow associated with the rotor tip leakage vortex.

The capability of the TURBO code to simulate the flow fields in both high speed axial and centrifugal compressors as well as to predict stall range extension will be assessed by comparison to experimental measurements obtained both with and without stall control technology in both a high speed axial compressor, Stage 35[1-5, 23] (Figure 1), and a high speed centrifugal compressor, CC3[6, 24], (Figure 2). The time-accurate simulations of these two high-speed compressors for which detailed experimental data are available provide assessment of the capability of the TURBO code for predicting the stall inception processes in a multistage axi-centrifugal compressor. The stage 35 and CC3 compressors were used in the development of the stall control technology, and as such provide an experimental database for validation of the unsteady simulations. Previous comparisons of the time-averages of unsteady phase-lag and partial annulus predictions to measurements have shown the validity of the TURBO code to capture the one-dimensional, and two-dimensional characteristics of these two compressors[11, 12].

The intent is to show sufficient evidence that the computational model reasonably captures the inherent behavior of compressors as they are throttled into stall rather than assuring that the model faithfully captures the exact
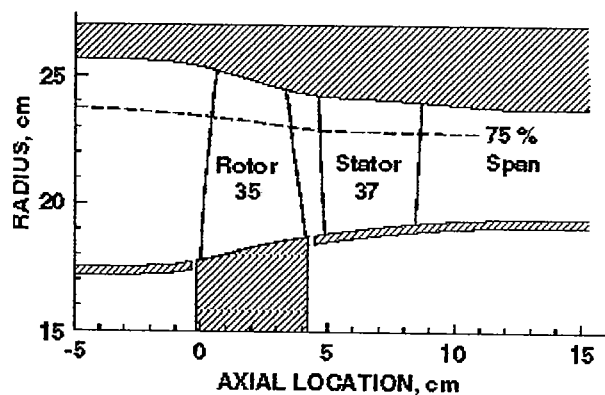
Figure 1 High-speed single stage axial compressor, Stage 35, validation case.
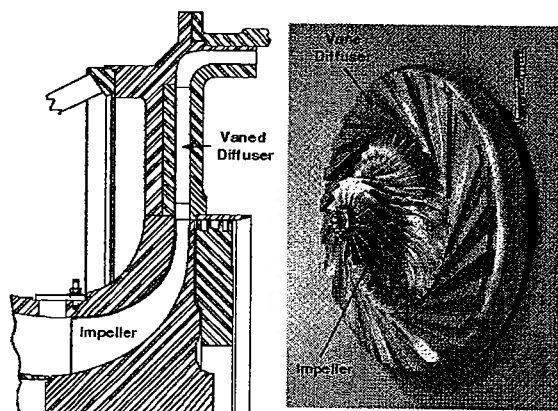

Figure 2 High-speed centrifugal compressor, CC3, validation case.

operational characteristics of the tested compressor. It is recognized that some features of the actual tested compressors are not captured by the computational model, for example the leakage gap at the rotor/stator hub interface, and the actual blade tip profile. Though these are certainly germane to how the actual tested compressor stalls they are not believed germane to understanding the fundamental stall inception characteristics of compression systems.

Stage 35 Results

The high-speed single-stage axial compressor, Stage 35, operating at 17189 RPM at design speed conditions (20.2 kg/sec) produces 1.82 total pressure ratio. This axial compressor consists of 36 rotor blades followed by 46 stator blades. To facilitate comparison of simulations with and without tip injection, the simulations of stage 35 used a three-blade-row grid as shown in Figure 3. This grid consists of an injector (blue), a rotor (pink), and a stator (green) blade row. The injector row has twelve injectors that are equidistant in the circumferential direction and each of these injectors are treated as a 'blade passage'. The injector grid is followed by the rotor grid, and then the stator grid. The grids are rotated and replicated around the annulus to generate a full-annulus grid, which incorporates all blade passages for each blade row. The effect of injection is modeled through addition of
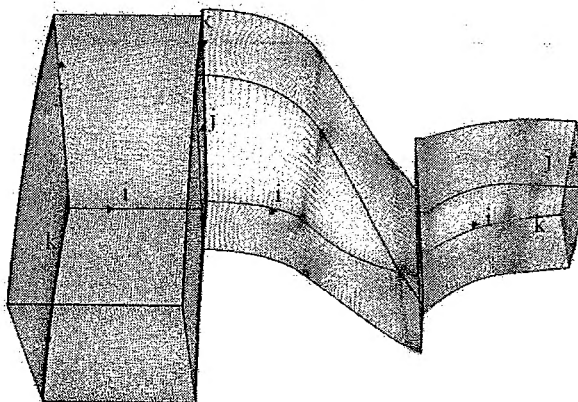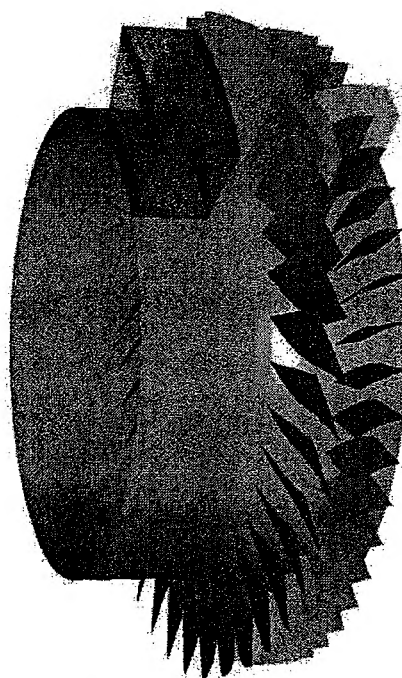

Figure 4 Three-blade-row Grid Model for the Stage 35 simulation

source terms in the injector grid. For the no-injection simulations the injection can be turned off by removing the source terms.

Stage 35 without Injection - This case was conducted to investigate the unsteady flow development of stall inception without stall control. During the stall inception process, stall cells can rotate around the annulus at speeds that are not necessarily multiples of the compressor rotational frequency, and therefore the assumption of both spatial and temporal periodicity is not valid. Thus, the only correct modeling technique is to compute the full-annulus of the compression system.

Compressor characteristics (speed lines) were generated by incrementally increasing the exit corrected mass flow boundary condition. A comparison of the TURBO predictions using full-annulus conditions to the experimentally measured design speed lines for Stage 35 is shown in Figure 4. The solid casing (no injection) case compares reasonably, with
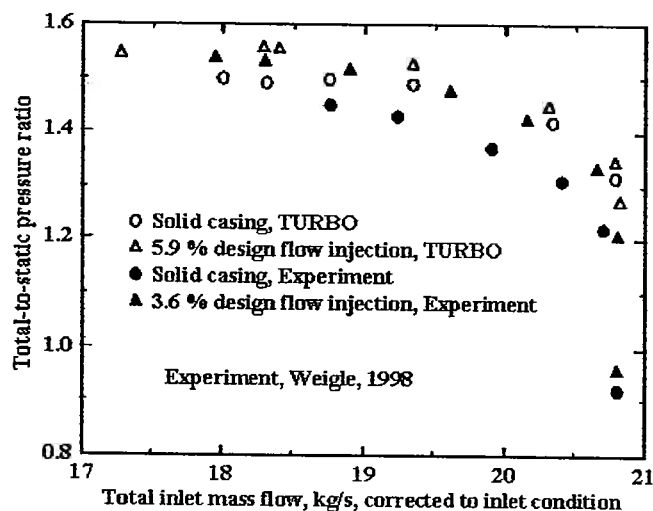
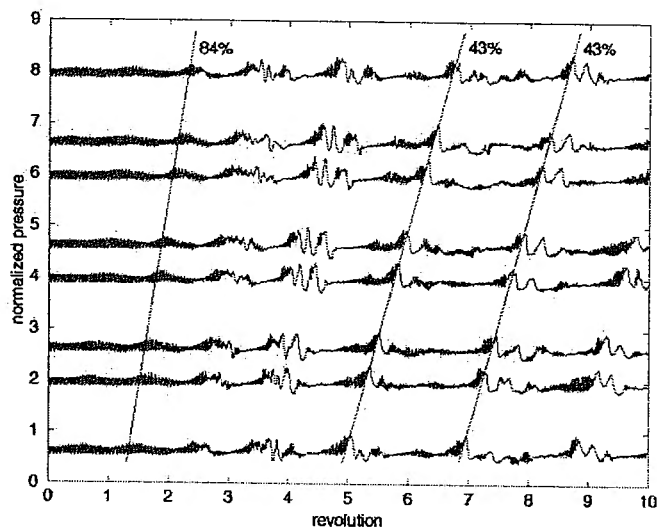**Figure 4 Stage 35 predicted and measured performance.**

Figure 5 Time history of static pressure variation at 8 locations around the annulus located 90% chord ahead of the rotor of Stage 35 without injection.
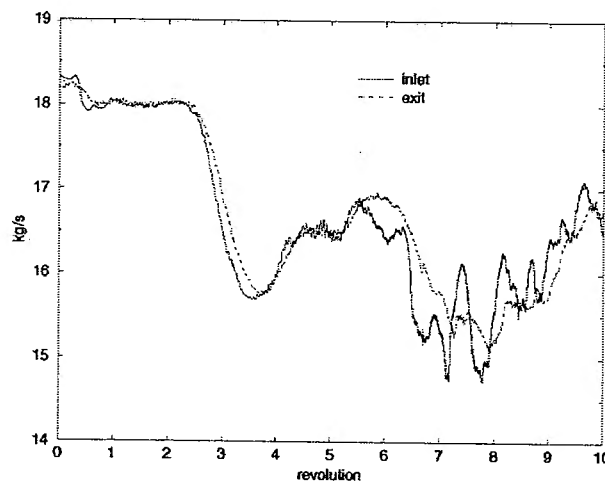
TURBO predicting higher pressure rise. These calculations used 328 CPUs for the full-annulus simulation.

In the stall inception simulation, eight numerical pressure probes were set up to record the unsteady pressure variation. The probes are located 90% chord upstream of the rotor leading edge at 98% span. They are arranged in 4 groups of two in order to fit in the 12 injectors. The circumferential locations are 10, 70, 100, 160, 190, 250, 280, and 340 degrees and are fixed in the absolute coordinate frame of reference. The time variation of pressure at the probe locations are shown in Figure 5, in which the pressure level is offset by the probe circumferential location. The normal axis, ordinate, thus correlates to the spatial distance of a traveling disturbance around the annulus. The stall condition was obtained by reducing exit corrected mass flow from 13.8 kg/s to 13.6 kg/s, corresponding to the last operating point in the speed line, Fig. 4.

Small, periodic pressure variations caused by the rotor blade passing can be seen in the first two revolutions in Fig 5 as the rotor passed by the probes. The stall cell, identified as the larger disturbance on top of the periodic variation was first detected at t=1.5T (T=time for one rotor revolution). It then grew in magnitude as it moved around the annulus with a speed indicated by the slope of the lines connecting the disturbances at various probes. The speed of the rotating stall cell started at 84% rotor speed and then slowed down to 43% in 4 revolutions. Inlet and exit mass flow history during the same period is shown in Figure 6 in which the mass flow remained relatively flat in the first two revolutions at 18 kg/s before it plunged sharply and then underwent some type of surge cycle.

In Figures 7, and 8 the entropy at a surface of revolution near the casing is shown at two instants in time. The full-annulus surface is illustrated by two half-annulus surfaces. At t=3.8T, Figure 7, the early phase of the stall inception, three separate high entropy (red color) regions can be seen with the axial extent covering from one chord upstream to just a little after the leading edges of the stator. The radial extent of the stall cell is shown in the axial cutting plane at 16 % chord before the rotor. Again the high entropy region shows the

Figure 6 Mass flow variation during stall inception process of Stage 35.

stall cell extending about 30% span from the casing. At t=10T, Figure 8, the stall cell evolves into the final stage as its rotating speed became stabilized. The three-cell stall has merged into a single-cell stall with the axial extent covering all the way from the inlet of the computation domain to after the trailing edge of the stator. The radial extent of the stall cell has now extruded about 70% span from casing.

The evolution of the simulated rotating stall cell is very similar to the spike stall inception mechanism described in several experiments [25, 26]. A common scenario for this stall inception process is that localized, three-dimensional pockets of instability in multiple rotor passages erupt first to form small sized multi-cell rotating stall. These stall cells move fast at the beginning and then merge into a single rotating stall cell within a few revolutions. The final speed of the consolidated stall cell is near half of the rotor speed [27].
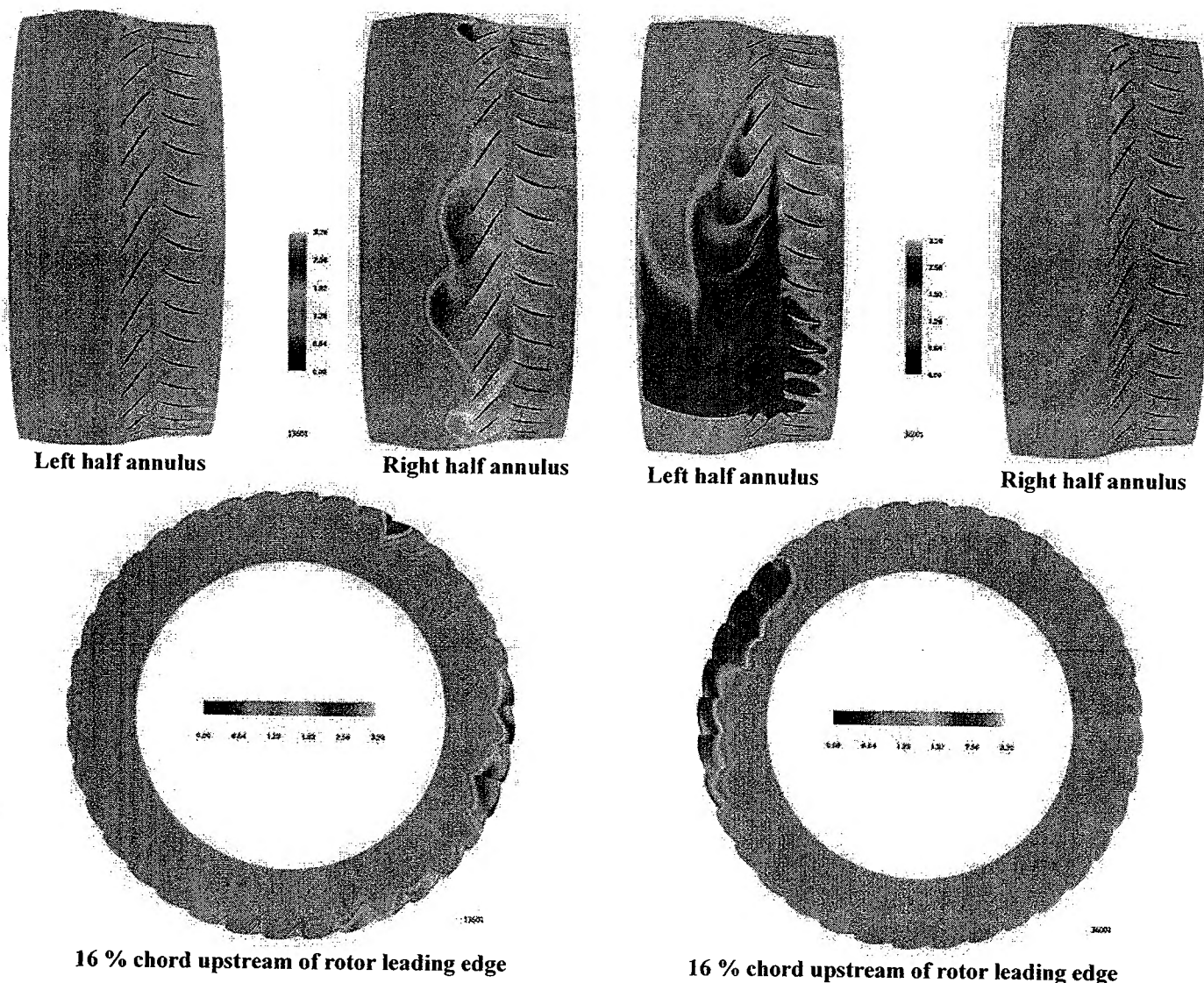
Left half annulus   **Right half annulus**

Left half annulus   **Right half annulus**

16 % chord upstream of rotor leading edge

16 % chord upstream of rotor leading edge

Figure 7 Entropy of Stage 35 during stall inception process, t=3.8T

Figure 8 Entropy of Stage 35 during stall inception process, t=10T

Stage 35 with Injection - One of the main topics addressed in the present investigation is the use of mass injection upstream of the rotor tip to increase the range of the compressor mass flow rates for which stable operation is possible. The injected flow is modeled by the addition of source terms equivalent to injection of 5.9% design mass flow (20.34 kg/s) or 1.2 kg/s downstream of the axial direction and with no yaw. This modeled injection is stronger than what was used in the experiment, which is 3.6% of the design flow.

The TURBO prediction of steady injection using full-annulus conditions is compared to the experimental measurement as shown in Figure 4. Total inlet mass flow in this figure is the sum of the inlet and injection flow, corrected to the inlet condition. Similar to the no-injection case, the overall performance compares reasonably, with TURBO predicting higher pressure rise. Both with and without injection cases choke at about 20.8 kg/s, which is about the same as the experiment. The predicted range extension measured by the difference of the lowest stable mass flow

between the injection and no injection cases, in relation to the no-injection stall flow rate, is 4%, compared to 4.3% in the experiment.

Figure 9 shows the entropy of the steady injection case on a surface of revolution near the casing. The plots are the instantaneous images taken from the same throttle setting as that of the no-injection case when stall occurred, for which the corrected exit mass was 13.6 kg/s. This corresponds to the second last operating point of the injection speed line in Fig. 4. This operating point is very close to the boundary of the compressor operation range that, without stall control, will develop into an unstable stall condition. Comparing these entropy plots with those of the no-injection case in Fig. 7, the overall entropy level is lower. But more importantly, the high entropy regions associated with the rotating stall cells in the no-injection case no longer exist. The steady tip injection effectively removes the stall cells at this throttle setting.

Axial velocity contours near the casing with and without injection are shown in Figure 10. In the no-injection case, Figure 10 b), reverse flows indicated by the negative axial

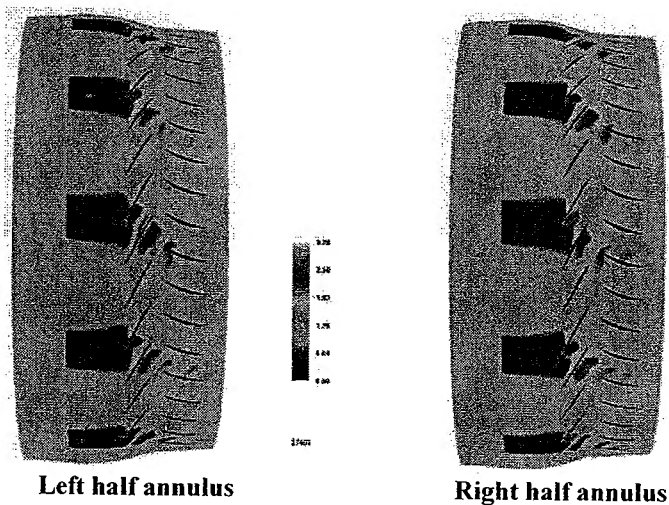Left half annulus   Right half annulus

Figure 9 Full-annulus unsteady simulation of stage 35 with tip injection showing contours of entropy which illustrate the impact of injection on the rotor flow field
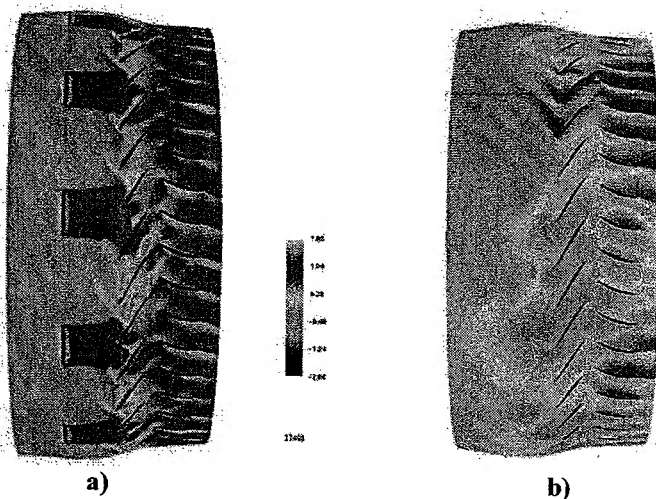

a)   b)

Figure 10 Axial velocity of Stage 35, a) with injection, and b) without injection

velocity (shaded by green) forms the three-cell rotating stall. The injected flows are seen as the high axial velocity ahead of the rotor in Figure 10 a), which corresponds to the low entropy regions in Figure 9. As shown in Figure 10 a), pockets of reverse flow appear near the suction surface of several rotor blades as they are outside of the influence of the injected flow. When the rotor blades enter the regions of the injected flows, much of the reverse flow was washed out. Equally interesting is that the pockets of reverse flow reappear as soon as the rotor blade moves out of the injector flow region. The fast 'kick back' of the reverse flow contributes to oscillation in flow field near the rotor leading edge. Pressure measurements at the eight probes shown in Figure 11 indicate spikes of small disturbance persistently appear on top of the periodic pressure oscillation, caused by the rotor passing, throughout the entire simulation. Samples of the eruption of the disturbance are illustrated by the dash lines in the figure, with their lifespan indicated by the length of the lines. Most of the disturbances are short-lived and
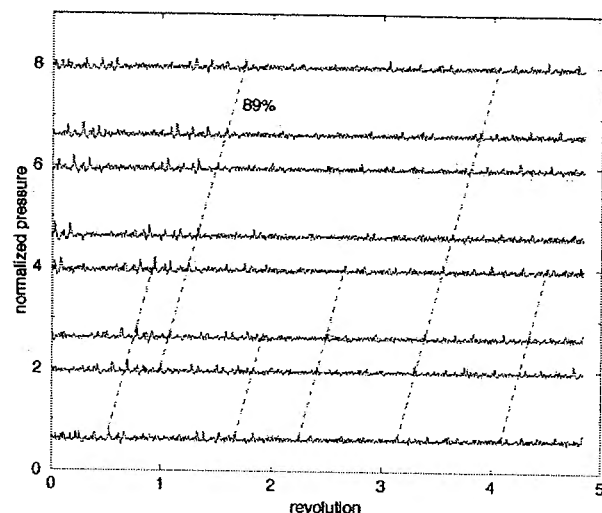

Figure 11 Pressure variation at 8 locations around annulus 90% chord ahead of the rotor of Stage 35 with injection

disappear within one rotor revolution. All of them move around the annulus at about 89% rotor speed. Since the probes are located between and outside the injectors, this indicates that the spike instability would spontaneously generate and grow the moment there is no injection to suppress it. Its magnitude remains small throughout the lifespan before being washed out by the next injector flow. This demonstrates that tip injection in this case does help in stabilizing the otherwise unstable flow, which when left uncontrolled will soon develop into a rotating stall.

Centrifugal Compressor, CC3

The high-speed centrifugal stage, CC3, operating at 21,789 RPM at design speed conditions (4.54 kg/sec) produces 4:1 pressure ratio. This centrifugal compressor consists of 15 main blades, 15 splitter blades for the impeller, followed by 24 diffuser vanes.

The simulations discussed herein are concerned with the CC3 High-Speed Centrifugal Compressor and its operation in the region near the onset of instability. Unsteady full-annulus simulations have been conducted both with and without external flow injection, which is used as a means of delaying the onset of compressor stall. These calculations used 315 processors for the full-annulus simulations. A similar grid model approach to what was used for the stage 35 simulations, see Fig. 3, was also used for the CC3 centrifugal compressor simulations with the exception that the injection model did not require an additional block as it was introduced as an injection boundary condition in the outer case flow path.

CC3 without Injection - As with the stage 35 no-injection case, this case was conducted to investigate the development of stall inception in a centrifugal compressor, however in this case the stalling element is the diffuser. Figure 12 is a plot of the predicted and measured overall compressor performance. A number of operating conditions, not all shown, have been
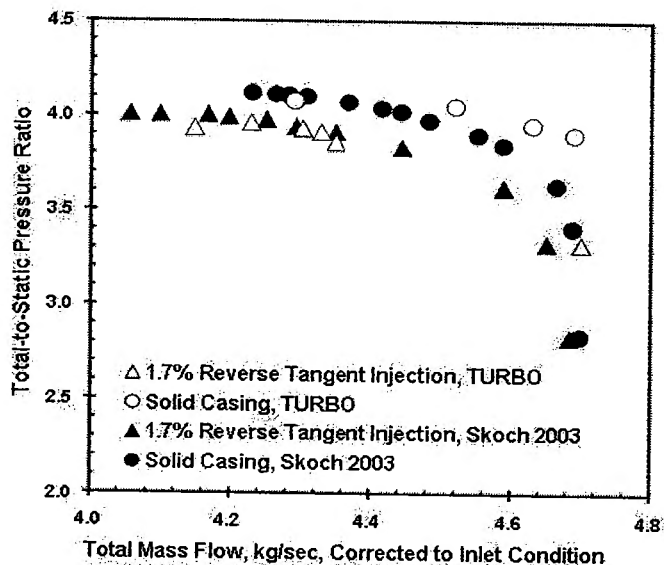
Figure 12 Predicted and measured performance of CC3. centrifugal compressor.

simulated in order to define the limit of stable operation of the compressor. The last stable operating condition, left most point, for the simulations was established using the exit corrected mass flow boundary condition. The final near stall "throttle setting" imposed via the exit corrected mass flow boundary condition was resolved to within 0.4 % of the stalling exit corrected mass flow boundary condition. All other predicted operating points shown in Figure 12 which are to the right of the last stable operating point were established using an exit static pressure boundary condition.

Figure 13 is an instantaneous snap-shot of the overall compressor (no injection) with velocity vectors shown only in the diffuser passages (in a grid plane very near the shroud). The velocity vectors are colored in terms of the relative Mach
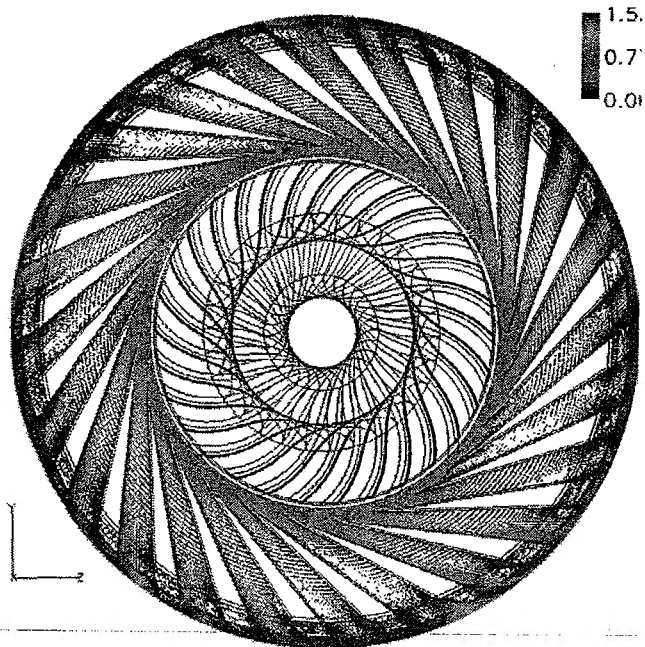

Figure 13 Diffuser flow field near shroud, no injection.

number; the maximum values are supersonic, which occurs near leading edge tip of the rotor blades. In this snap-shot figure, one diffuser passage is showing reverse flow at its entrance. This passage is slightly to the left of the 12 o'clock position. Another passage near the 5 o'clock position shows some mild evidence of reverse flow at its entrance. Other than these two, the remaining passages look well established with flow in the correct direction. At a different instant in time different passages show evidence of reverse flow. The stalling passages rotate around the annulus with time.

Figure 14 a) is a blown-up view (again near the shroud) of the reverse flow passage in Figure 13. Velocity vectors in the rotor passages and their exit regions are relative to the blade motion. The two neighboring passages look to be unaffected. This particular case appears to be operating just at the edge of the stability limit; one diffuser passage is obviously stalled. This is consistent with what has been
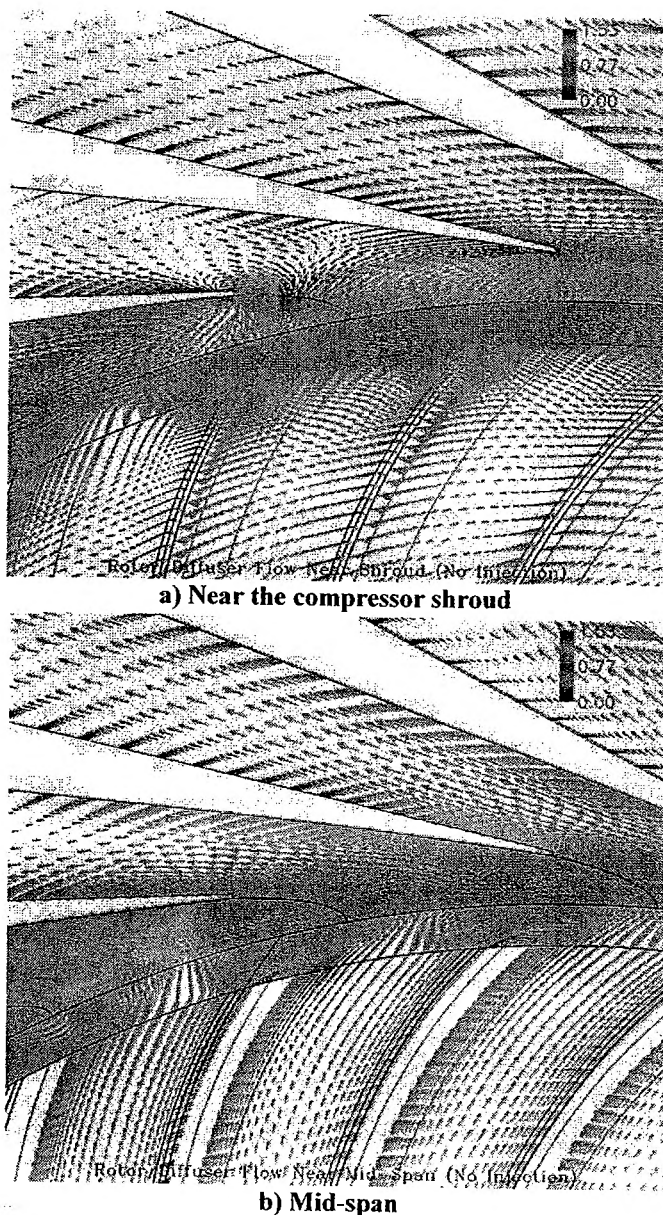

a) Near the compressor shroud

b) Mid-span

Figure 14 Blow up of instantaneous snap-shot of diffuser flow field at near stall condition, no injection.

measured experimentally in the CC3 compressor using digital particle image velocimetry[28]. The simulation is stable though as the physical exit flow rate, as well as the compressor static-to-total pressure ratio have held steady at values of 4.29 kg/sec (9.43 lbm/sec), and 4.07, respectively, for the last 4-5 rotor revolution periods of the simulation. Figure 14 b) is the same view as Figure 14 a) but at a plane near mid-span. No evidence of flow reversal is seen suggesting that any such problems are confined to the near-shroud region.

CC3 with injection - Figure 15 is the same type of view as shown in Figure 13 in the previous paragraph. However in this case there are eight passages with injection air supplied at the passage entrance. These injection "ports" can be seen as the dark-colored spots near the leading edge of the diffuser vanes. As before, the grid plane is very close to the shroud. Figure 16 a) is a blown-up view of the exact same passage as the one discussed in the previous paragraph, Figure 14 a). Keep in mind the relative velocity vectors in the rotor passages and exit regions. In this case, the passage is sandwiched between two passages containing injection ports. Though the entrances of the injector passages are noticeably distorted, the sandwiched passage is flowing well. Moving inward toward the mid-span Figure 16 b), the flow in the injector passages is seen to be much improved. The physical exit flow rate has converged at approximately 4.15 kg/sec (9.13 lbm/sec) with static-to-total pressure ratio 3.92. The simulation was converged for 4-5 rotor revolutions wherein the values held steady with no indications of stalling.
The results shown demonstrate the effect of the injection on the flow field; the curves in Figure 12 also show that some extension in the operating range has been achieved. The computed flow rates for the left-most points on these curves do not match the experimental results 4.22 kg/sec (9.28 lbm/sec) without injection, 4.05 kg/sec (8.9 lbm/sec) with
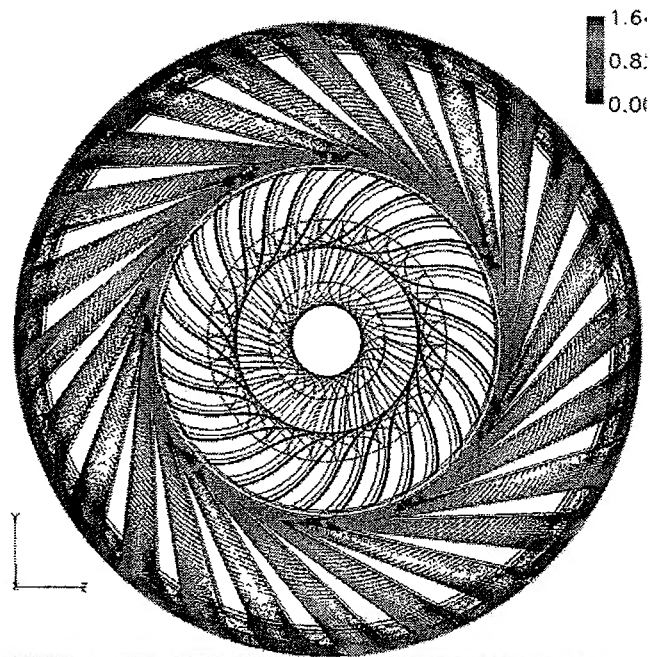
injection). However, the difference in the two flow rates (i.e., non-injection versus injection) compare rather well with the computed difference being 0.14 kg/sec (0.3 lbm/sec), and the experimental difference being 0.17kg/sec (0.38 lbm/sec).

The disagreement in the actual flow rate values may be due in part to relatively poor grid quality at the diffuser vane leading edges which perhaps excessively blunted the vane leading edges. However, the flow-rate difference matches reasonably well, and this gives an indication that the computed range extension is comparable to that of experiment. So, the computational application of injection at the shroud of the diffuser entrance seems to show very similar benefits as that of experiment. Recent experimental results[29] have shown that injection applied on the hub side at the leading edge of the diffuser vanes provides very little, if any, benefit to compressor performance.
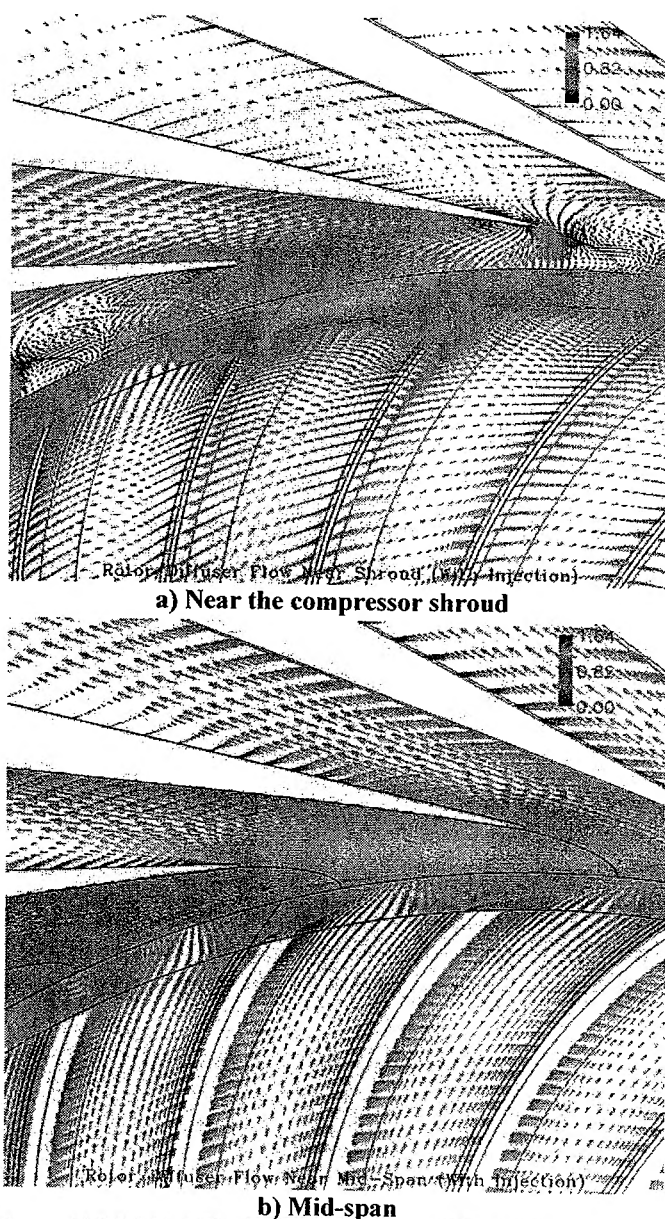

a) Near the compressor shroud

b) Mid-span

Figure 16 Blow up of instantaneous snap-shot of diffuser flow field at near stall condition, with injection.

Figure 15 Diffuser flow field near shroud, with injection.

Discussion and Conclusions

The unsteady full-annulus simulations of the high speed axial and centrifugal compressor validation cases show good agreement with measurements. The simulation results of the high speed axial compressor case provide evidence of the capability of such codes for predicting the onset of flow instabilities and their subsequent growth into a fully developed rotating stall. The simulation results clearly show multiple stall cells traveling at about 84% of rotor speed which then coalesce into a larger single stall cell that rotates at about 43% of rotor speed. This is consistent with what has been observed experimentally.

In addition, the simulations predict the beneficial impact of stall control technology, injection of high relative total pressure fluid ahead of the rotor leading edge tip at discrete locations around the annulus. As evidenced from the simulation results, the stall control technology appears to suppress the growth of the instabilities, thereby providing enhanced compressor stability.

Similarly, the unsteady full-annulus simulations of the CC3 centrifugal compressor stage also indicate the development of stalling passages with reverse flow regions as has been observed experimentally in the CC3 compressor. The beneficial impact of the reverse tangent stall control technology applied at discrete locations around the annulus in the diffuser vaneless space is also clearly predicting enhanced stability, as has been measured experimentally.

Further interrogation of these simulations is expected to provide insight into the flow physics of the stall inception process of these compressors, both with and without stall control technology. Such insight is expected to provide improved design guidelines for extending the stable operating range of compressors.

Acknowledgements

References

1. Suder, K.L., Hathaway, M.D., Thorp, S.A., Strazisar, A.J., and Bright, M.M., "Compressor Stability Enhancement Using Discrete Tip Injection," *ASME Journal of Turbomachinery*, Vol. 123, pp. 14-23, January 2001.

2. Weigl, H.J., Paduano, J.D., Frechette, L.G., Epstein, A.H., Greitzer, E.M., Bright, M.M., and Strazisar, A.J., "Active Stabilization of Rotating Stall and Surge in a Transonic Single Stage Axial Compressor," *ASME Journal of Turbomachinery*, Vol. 120, No. 4, pp. 625-636, 1998.

3. Spakovszky, Z. S., Weigl, H. J., Paduano, J. J., van Schalkwyk, C. M., Suder, K. L., Bright, M. M., "Rotating Stall Control in a High-Speed Stage with Inlet Distortion: Part I - Radial Distortion," *ASME Journal of Turbomachinery*, Vol. 121, pp.510-516, July 1999.

4. Spakovszky, Z. S., J. J., van Schalkwyk, C. M., Weigl, H. J., Paduano, Suder, K. L., Bright, M. M., "Rotating Stall Control in a High-Speed Stage with Inlet Distortion: Part II - Circumferential Distortion," *ASME Journal of Turbomachinery*, Vol. 121, pp.517-524 July 1999.

5. Strazisar, A. J., Bright, M. M., Thorp, S., Culley, D. E., Suder, K. L., "Compressor Stall Control Through Endwall Recirculation," ASME Paper No. GT2004-54295, June 2004.

6. Skoch, G. J., "Experimental Investigation of Centrifugal Compressor Stabilization Techniques," *Journal of Turbomachinery*, October, 2003, pp. 705-713.

7. Hoying, D.A., Tan, C.S., Vo, H.D., and Greitzer, E.M., "Role of Blade Passage Flow Structures in Axial Compressor Rotating Stall Inception," ASME Paper No. 98-GT-588, June 1998.

8. Gong, Y., Tan, C.S., Gordon, K.A., and Greitzer, E.M., "A Computational Model for Short Wavelength Stall Inception and Development in Multistage Compressors," ASME Paper No. 98-GT-476, June 1998.

9. Davis, R. L., Yao, Jixian, "Prediction of Compressor Stage Performance From Choke Through Stall," AIAA-2005-1005, presented at the 43rd AIAA Aerospace Sciences Meeting, Reno, NV, January 2005.

10. Saxer-Felici, H.M., Saxer, A., Ginter, F., Inderbitzin, A., and Gyarmathy, G., "Structure and Propagation of Rotating Stall in a Single Multistage Axial Compressor," ASME Paper No. 99-GT-452, June 1999.

11. Hathaway, M. D., Chen, J., Webster, R., "Time Accurate Unsteady Simulations of the Stall Inception Process in the Compression System of a U.S. Army Helicopter Gas Turbine Engine," 2003 DoD High Performance Computing Modernization Program User's Group Conference, Bellevue, Wa., June, 9-13, 2003.

12. Hathaway, M. D., Chen, J., Webster, R., Herrick, G. P. "Time Accurate Unsteady Simulations of the Stall Inception Process in the Compression System of a U.S. Army Helicopter Gas Turbine Engine," 2004 DoD High Performance Computing Modernization Program User's Group Conference, Williamsburg, VA., June, 7-10, 2004.

13. Van Zante, D.E., Strazisar, A.J., Wood, J.R., Hathaway, M.D., and Okiishi, T.H., "Recommendations for Achieving Accurate Numerical Simulation of Tip Clearance Flows in Transonic Compressor Rotors,"

ASME Journal of Turbomachinery, Vol. 122, pp. 733-742, October 2000.

14. Chen, Jen Ping and Barter, Jack, "Comparison of Time-Accurate Calculations for the Unsteady Interaction in Turbomachinery Stage," AIAA Paper No. AIAA-98-3293, July 1998.

15. Adamczyk, J. J., "Model Equation for Simulating Flows in Multistage Turbomachinery," ASME Paper No. 85-GT-226. 1985.

16. Chen, J.P., Celestina, M. L., and Adamczyk, J. J., "A New Procedure for Simulating Unsteady Flows Through Turbomachinery Blade Passages," ASME Paper No. 94-GT-151, June 1994.

17. Shabbir, A., Zhu, J., and Celestina, M., "Assessment of Three Turbulence Models in a Compressor Rotor," ASME Paper No. 96-GT-198, June, 1998.

18. Chen, J.P. and Briley, W.R., "A Parallel Flow Solver for Unsteady Multiple Blade Row Turbomachinery Simulations," ASME Paper No. 2001-GT-348, June 2001.

19. Remotigue, M.G., "A Pre-Processing System for Structured Multi-Block Parallel Computations", Numerical Gd Generation in Computational Field Simulations, Proceedings of the 8th International Conference held at Honolulu, Hawaii, June 2002.

20. Pankajakshan, R. and W. R. Briley, "Parallel Solution of Viscous Incompressible Flow on Multi-Block Structured Grids Using MPI", Parallel Computational Fluid Dynamics - Implementations and Results Using Parallel Computers, Edited by S. Taylor, A. Ecer, J. Periaux, and N. Satofuca, Elsevier Science, B. V., Amsterdam, pp. 601-608, 1996.

21. Pankajakshan, R., Taylor, L. K., Jiang, M., Remotigue, M.G., Briley, W. R., and D. L. Whitfield, "Parallel Simulations for Control-Surface Induced Submarine Maneuvers," AIAA Paper 2000-0962, 38th Aerospace Sciences Meeting, Reno, NV, 2000.

22. Pankajakshan, R. and W. R. Briley, "Parallel Flow Simulations for Appended Submarines with Rotating Propulsors," High Performance Computing: Contributions to DoD Mission Success 1998, (DoD HPCMO) p. 61, 1998

23. Reid, L., and Moore, R. D., 1978, "Performance of Single-Stage Axial-Flow Transonic Compressor with Rotor and Stator Aspect Ratios of 1.19 and 1.26, Respectively, and With Design Pressure Ratio of 1.82," Tech., Rep. TP-1338, NASA. Nov. 1978.

24. McKain, T. F., and Holbrook, G. J., 1982, "Coordinates for a High Performance 4:1 Pressure Ratio Centrifugal Compressor," NASA Contractor Report No. 204134.

25. Day, I. J., "Stall Inception in Axial Flow Compressors," ASME Journal of Turbomachinery, Vol. 115, pp. 1-9

26. Camp, T.R. and Day, I. J, "A Study of Spike and Modal Stall Phenomenoa in a Low-Speed Axial Compressor," ASME Journal of Turbomachinery, Vol. 120, pp. 393-401.

27. Cumpsty, N.A., "Compressor Aerodynamics," Krieger Publishing Co., 2004.

28. Wernet, M. P, Bright, M. M., Skoch, G. J. "An Investigation of Surge in a High-Speed Centrifugal Compressor Using Digital PIV," *ASME Journal of Turbomachinery*, Vol. 123, pp. 418-428, April 2001.

29. Skoch, G. J., 2005, "Experimental Investigation of Diffuser Hub Injection to Improve Centrifugal Compressor Stability," *ASME Journal of Turbomachinery*, Vol. 127, pp. 107-117.